Search-Lidar Demonstrator for Detection of Small Sea-Surface Targets

Johan C. van den Heuvel, Herman H.P.Th. Bekman, Frank J.M. van Putten, Leo H. Cohen, Ric (H.) M.A. Schleijpen
TNO Defence, Security and Safety, Oude Waalsdorperweg 63, The Hague, The Netherlands

ABSTRACT

Coastal surveillance and naval operations in the littoral both have to deal with the threat of small sea-surface targets. These targets have a low radar cross-section and a low velocity that makes them hard to detect by radar. Typical threats include jet skis, FIAC's, and speedboats. Lidar measurements at the coast of the Netherlands have shown a very good signal-to-clutter ratio with respect to buoys located up to 10 km from the shore where the lidar system was situated. The lidar clutter is much smaller than the radar clutter due to the smoothness of the sea surface for optical wavelengths. Thus, almost all laser light is scattered away from the receiver. These results show that due to the low clutter a search lidar is feasible that can detect small sea-surface targets. A search-lidar demonstrator is presented and experimental results near the coast of Holland are presented. By using a high rep-rate laser the search time is limited in order to be useful in the operational context of coastal surveillance and naval surface surveillance. The realization of a search lidar based on a commercially available high power and high rep-rate laser is presented. This demonstrator is used to validate the system modeling, determine the critical issues, and demonstrate the feasibility.

Keywords: Laser, laser range finder, small targets, lidar, detection

INTRODUCTION

Detection of small sea-surface targets, like periscope tubes, jet skis, swimmers and small boats, is important both for civil and naval scenarios, e.g. 'man overboard', illegal immigration, drugs transport and asymmetric threats. However, the detection of these targets using current radar systems is difficult due to the small radar cross-section and low velocity of these targets and the presence of strong radar clutter from the sea surface.

The detection of sea-surface targets by lidar is based on the low reflection of laser light by the sea and the strong reflection of hard targets. Experiments from the "Meetpost Noordwijk" near the coast of the Netherlands (in 1996 and 2000) and along the Irish west coast during the PARFORCE trials[1] in 1999 and 2000 confirmed the low sea reflection. Other experiments learned that relatively strong signals were returned from small hard targets, e.g. poles and streetlamps, a principle that is used by laser range finders.[2]

Lidar systems are particularly suitable as a search-around system for the detection of small targets at the sea surface. Their small instantaneous field-of-view, small pulse durations and high power combine a high spatial resolution with a large detection range. Moreover, it is shown here that small sea-surface targets give strong reflections in comparison with the reflection from the sea surface. This results in a large signal-to-clutter ratio. Operation during periods of radio silence is possible since detection of optical radiation with standard radio equipment is not possible. Laser radiation can only be detected with special equipment, e.g. laser warning systems.

The maximum detection range of a search lidar depends not only on the system properties but also on the atmospheric condition. The latter plays a dominant role, especially under low visibility conditions because both the transmitted laser radiation and the backward reflected radiation are attenuated. Consequently, the maximum detection range depends on the system properties, on the target reflection properties, and on the atmospheric visibility.

Laser Radar Technology and Applications XIII, edited by Monte D. Turner, Gary W. Kamerman
Proc. of SPIE Vol. 6950, 69500W, (2008) · 0277-786X/08/$18 · doi: 10.1117/12.777947

Search lidars are intended for the detection of targets and measurement of their position. Speed and heading can be obtained from multiple measurements. It is possible that search lidars can also be used for classification or identification of non-cooperating long-range targets.

The principle of a search lidar consists of a scanning laser beam with a relatively small instantaneous field-of-view (IFOV) in combination with an optical receiver, aligned with the laser beam. Scanning is done in azimuth and elevation to cover the sea surface around the ship. The receiver measures part of the backward-scattered laser radiation from targets within the IFOV of the laser beam. Range information is obtained by using pulsed lasers in combination with a receiver that records the time-of-flight of the received laser pulse. A sketch of a basic search lidar is shown in Figure 1 with diagrams of the scanning system and the interaction at the sea surface.

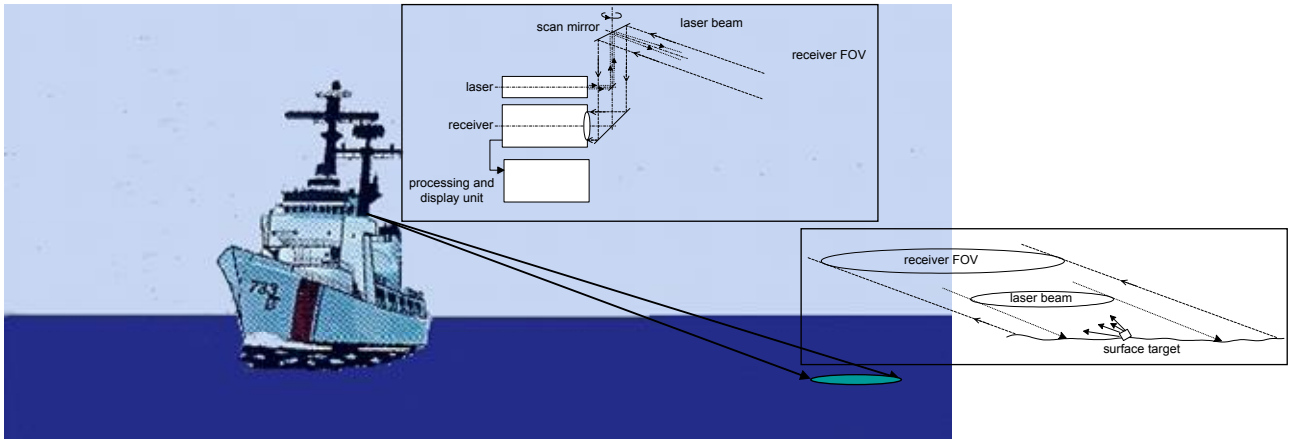

Figure 1: Sketch of a search lidar with diagrams of scanning system and sea-surface interaction.

The reflection of the sea surface is very important in this context, but theory is complex, difficult to handle and commonly used to predict reflections from the sun and the sky towards an observer but not to predict reflections of mono-static lidar systems or laser range finders. Therefore, instead of trying to calculate the reflection, we have measured the target and the sea reflection with our backscatter lidars at 1.06 µm and 1.57 µm near the Dutch coast.

The design and experimental results of a search-lidar demonstrator is presented in this paper. It is shown that such a system is feasible with current laser technology and can provide a range of 2 km with a low power laser and a corresponding search time of a few seconds. With a laser of higher power, ranges near 10 km have shown to be feasible.

EXPERIMENTAL SET-UP

To verify the search lidar concept, initial measurements were carried out on small buoys near Scheveningen harbor (North Sea coast, The Netherlands) at distances between 1 and 10 km with the 1.06 µm system at a pulse energy of 20 mJ at 20 Hz (system 1). Although the lidar operating at 1.06 µm is an excellent tool for a feasibility study, it is not eye-safe. Therefore, an eye-safe lidar has been developed operating at a wavelength of 1.57 µm (system 2), which is absorbed in the eye and not focused on the retina. It is possible that the reflection properties of surfaces and the scattering properties of atmospheric particles at the eye-safe wavelength will be different from the 1.06 µm wavelength. However, different references indicate that the differences are marginal.[3,4,5,6] Molecular transmission of the atmosphere calculated with Modtran showed that under normal atmospheric conditions the transmission at 1.06 µm and 1.57 µm is comparable. Therefore, no special molecular effects are expected. The relatively strong absorption lines at 1.1 µm and 1.4 µm are caused by water vapor but are outside the applied laser wavelengths.

The lidar system at 1.57 µm is depicted in Figure 2. The green box contains the OPO laser wavelength converter, which converts the pump laser wavelength of 1.06 µm into the more eye-safe wavelength of 1.57 µm.[7,8,9] The white box on top

of the green box contains the receiver telescope and the detector. The white box right next to the green box is the 1.06 μm pump laser.

The pump laser for the OPO is a Q-switched Nd:YAG laser. The maximum output is 350 mJ per pulse with a pulse length of 5 ns at a rep-rate of 20 Hz. In the OPO the laser radiation at 1.06 μm is converted to 1.57 μm. The conversion takes place in a non-linear crystal. To increase the non-linear conversion efficiency, it is beneficial to increase the laser power density by focusing the laser beam into the crystal. However there is a limit on the maximum power density that the crystal can withstand.

Figure 2: 1.5 micron lidar system

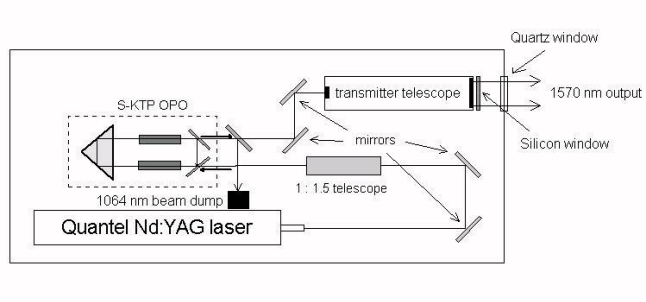

Figure 3: Optical layout of eye safe lidar transmitter.

We have made an OPO design that maximizes the non-linear conversion efficiency by using two crystals instead of one, and by using S-KTP instead of KTP crystals, which have a higher damage threshold.[Error! Reference source not found.,11] We ended up with a ring cavity design. The OPO laser is connected to an optical telescope and in addition some filters are placed in the beam line to completely block the eye-hazardous laser pump light. The layout of the transmit section of the lidar is shown in Figure 3. The lidar system was operated with maximum pump pulse energy of 205 mJ at a rep-rate of 10 Hz. The output from the transmitter at 1570 nm was around 30 mJ.

In order to demonstrate the feasibility of a search-lidar, a new demonstrator system was constructed around a high rep-rate laser. The laser from Photonics Industries runs at a pulse repetition rate up to 3 kHz; power output is 2 W at 1 kHz with a pulse energy of 2 mJ; wavelength is 1516 nm; pulse width is 15 ns at 1 kHz; beam quality is nearly diffraction limited (M^2<1.2) with a beam diameter of 0.9 mm (system 3).

The detector electronics is based on a InGaAs APD of 80 um with 200 MHz bandwidth with a noise level of 220 fW/√Hz. The APD is connected to a logarithmic amplifier with a gain of 40 dB. The timer module is based on a National Instruments NI 6602 PCI board with an 80 MHz timer. With this board a distance resolution of 2 meter is achieved.

The receiver optics consists of a Cassegrain telescope with a focal length of 750 mm and an aperture of 125 mm. Unfortunately, there is a large mismatch between the receiver FOV of 0.1 mrad and the laser beam divergence. The FOV of the receiver is enlarged by an aspheric lens close to the detector, see Figure 4. Focal length of the asphere is 3.1 mm. A disadvantage is the critical alignment and large lens distortion. By using a negative lens before the asphere the lens distortion is reduced and the alignment tolerance is improved.

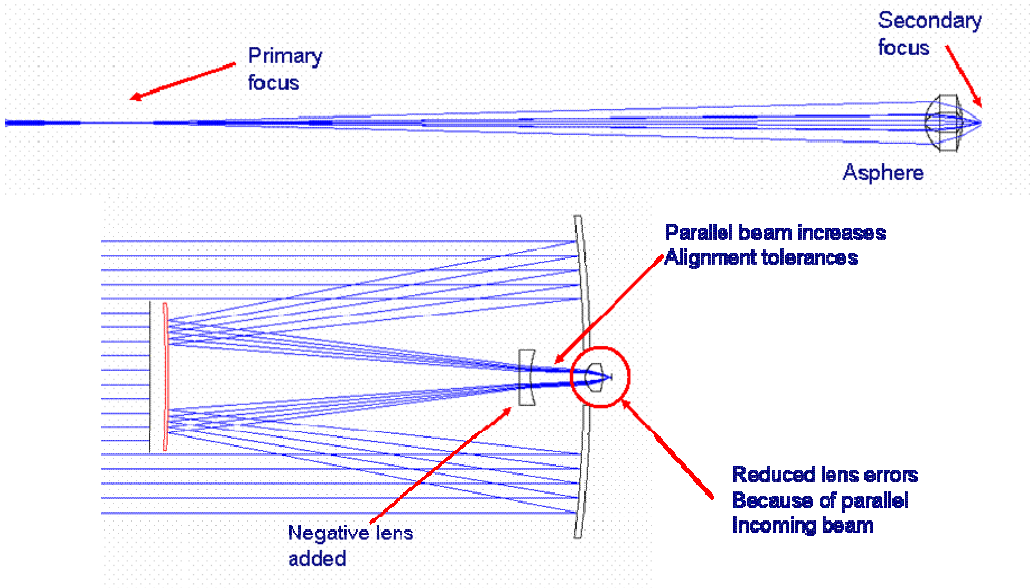

Figure 4: Principle and Cassegrain implementation of FOV enlargement.

The laser-receiver assemble is mounted on a rapid pan-tilt unit of Instro model Mantis. This unit has a maximum payload of 150 kg; an elevation and azimuth range of 90 and 360 degrees; a maximum velocity of 50 deg/s; a maximum acceleration of 100 deg/s^2. The accuracy of positioning is 1 mrad. The unit is controlled by a computer through a RS422 computer interface. Figure 5 shows the sensor head and computer interface. The interface module (yellow block) provides a stop pulse to the timer in the absence of a laser echo.

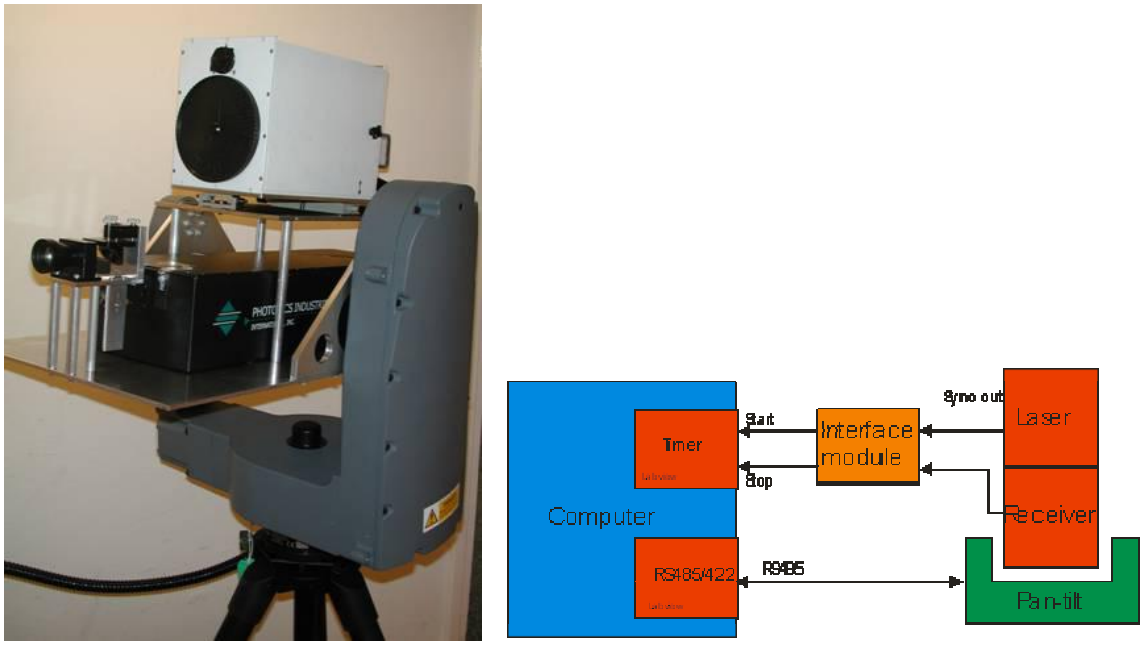

Figure 5: Sensor head with laser and receiver on the left and computer interfacing on the right.

During the first day of testing the complete system, the laser failed due to damage of the cavity optics. In order to test the system, the high power high rep-rate laser was replaced by a low power high rep-rate laser. The pulse energy of this laser was only 7 μJ and the maximum range was severely limited because of this. However, system tests were possible with this laser. In addition, this laser could be an interesting option for shorter range detection systems, since it leads to a

much cheaper system and also to a more compact one. Figure 6 shows two photographs of the system in operation at the coast of Holland (system 4).

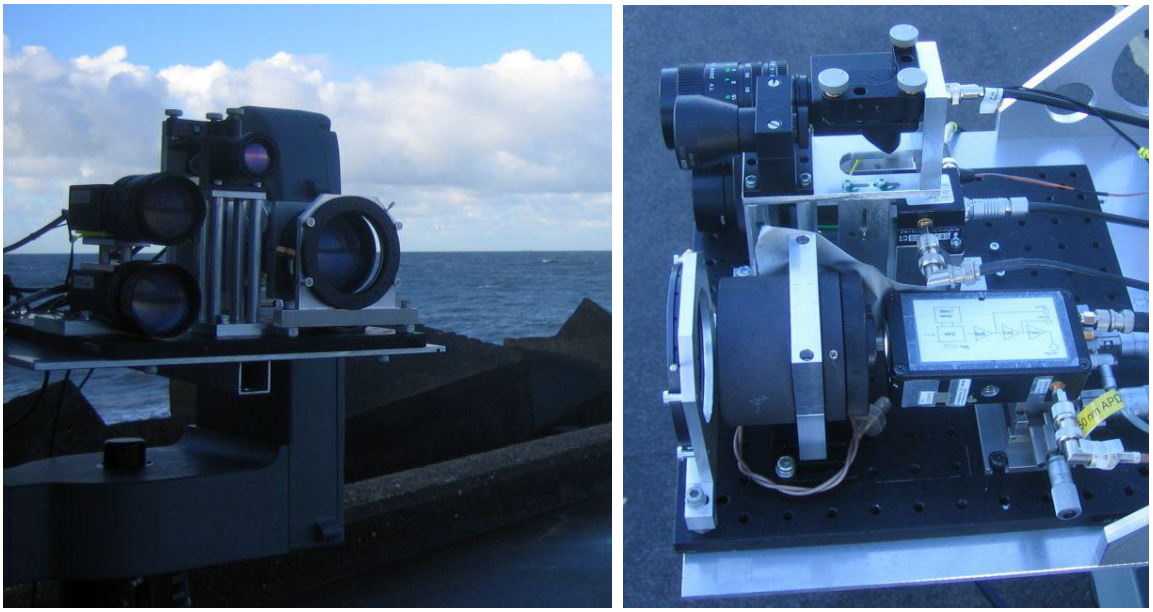

Figure 6: Modified sensor head with a small laser.

EXPERIMENTAL RESULTS

A suitable location with small sea-surface targets was searched along the Dutch coast, to investigate the principle of detecting small targets at the sea surface. The location of interest should have some small objects in the water, preferably at least several kilometers from the observation point. A good location appeared to be the southern Scheveningen harbor pier with a length of about 600 m at approximately (52°6'N; 4°15'E). From this position several buoys at distances between 1 km and 10 km are visible.

A magnified portion of Hydrographic Map 1801.7 is shown on the left of Figure 7. The map (courtesy Royal Netherlands Navy, 'Dienst der Hydrografie') shows the buoys near the Scheveningen harbour entrance. The rectangles in the background of the map are approximately 1x2 km^2. The lidar was positioned at the end of the southern pier, near the green traffic light (near text 'Obtns'). Shown on the right side of Figure 7 is a view over the sea in NW direction from the southern harbour pier, with the lidar in the front and the buoys in the back. Red circles mark the four buoys of interest that are from left to right: Dr-B, Drain-W, Dr-A, and Drain-E. The ranges of the buoys are Dr-B at 1.4 km, Drain-W at 1.9 km, Dr-A at 1.2 km, and Drain-E at 1.6 km.

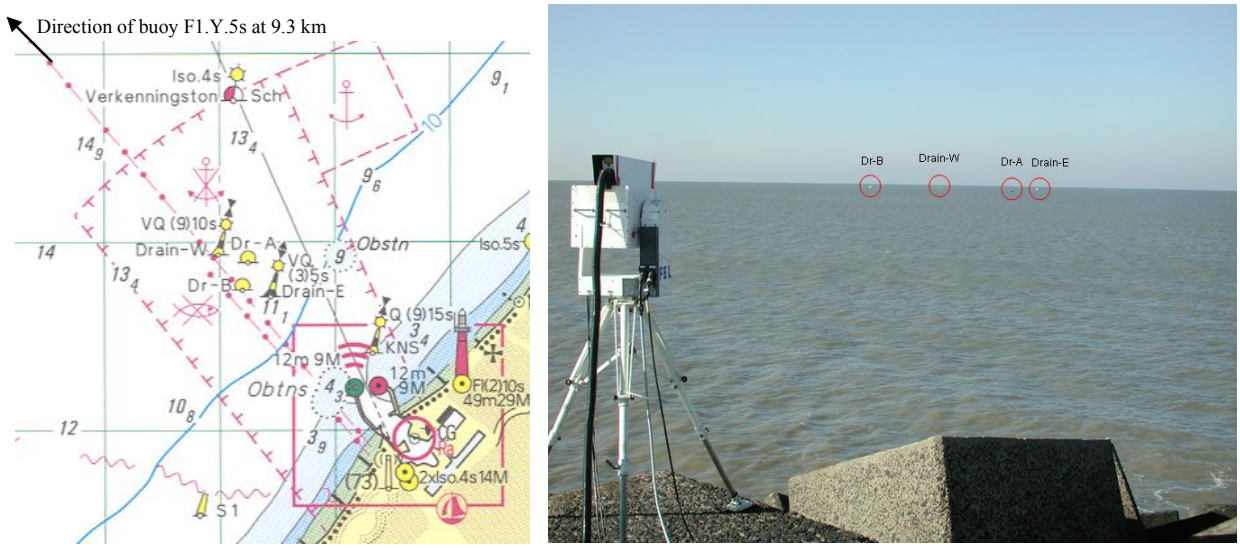

Figure 7: Magnified portion of Hydrographic Map 1801.7 (left) and the lidar situated at the end of the southern pier (right).

The lidar at 1.06 μm (system 1) was set up at the end of the southern Scheveningen harbor pier at about 500 m from the surf zone and the measurements were carried out in north-westerly directions towards open sea. No shipping traffic was observed during the experiments. The weather conditions were good. Cloudless sky, wind speed 6-7 m/s, wind direction 70 degrees, air temperature 12 °C and air pressure 1031 hPa. The water temperature was not specified in the weather report, but based on previous information in this time of the year it is assumed that the water temperature is about 16 °C. The wave height was about 0.5 m and whitecaps were only occasionally observed.

Horizontal lidar measurements were carried out at 10 different elevation angles from +0.46° degrees down to –0.49° to observe buoy reflections at different heights. Results obtained from one of these measurements under the elevation angle of –0.24° are presented in Figure 8. The lidar is in the right most position in this figure. Reflections from the buoys are indicated with red circles. Distances between the concentric range indicators are 500 m. The regular fringes at ranges larger than 2 km (in the most left part in the figure) are reflections from the wave tops. The graph at the bottom is plotted with the same data but with another color scale showing only the strong reflection from the buoys.

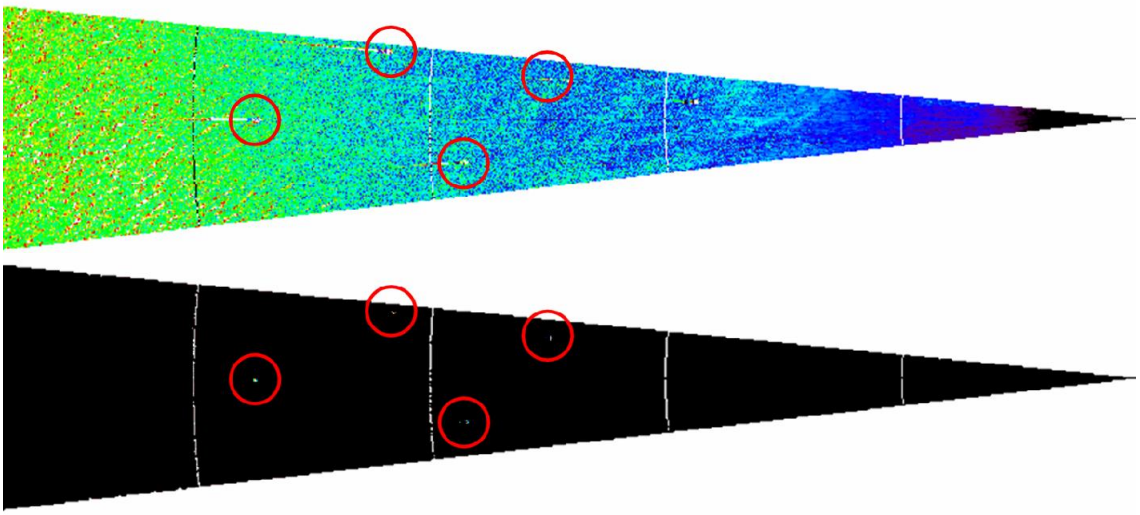

Figure 8: Results of a horizontal lidar scan over an azimuth angle interval of 12 degrees and at an elevation angle of –0.24°. Two color scales are used. The top graph emphasizes the atmospheric backscatter while the bottom graph shows only the strong reflection from the four buoys.

During later experiments, the lidar could successfully measure the position and reflection of the buoy F1.Y.5s in northwesterly direction at a distance of 9.3 km. The latter could not be observed with the naked eye under these prevailing conditions and only slightly using a binocular. Using the lidar, the buoy could be detected with a signal-to-noise ratio of about 140. A screen snapshot of the waveform recorder is shown in Figure 9. The lidar waveform presented in Figure 9 was recorded with a time base of 10 µs/div and a pretrigger of 10 µs. The gradual decrease in the signal between about 10 µs and 60 µs represents the atmospheric backscatter, attenuated by the geometric effect and the atmospheric transmission losses. Due to the application of an analog logarithmic amplifier, which suppresses large signal amplitudes and enhances low signal amplitudes, the large dynamic range of the signal could be covered within a single waveform. The relatively strong peak, visible at 62 µs after the pretrigger, comes from the buoy at 9.3 km from the lidar.

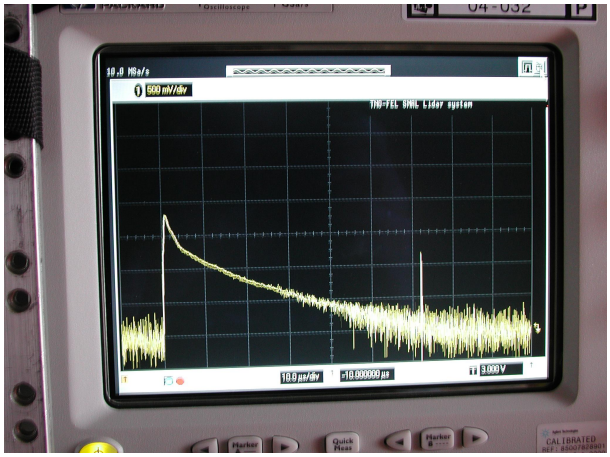

Figure 9 Photo of the oscilloscope screen with a lidar waveform showing the reflected signal from buoy Fl.Y.5s at 9.3 km.

The 1.5 µm lidar (system 2) that was presented in the previous section was used at the same location as the 1.06 µm (but a year later) to check whether the same favorable results could be achieved at this eye-safe wavelength. Since this system does not have a logarithmic receiver for the atmospheric return signal, we can only show the linear plot of the return of the buoys. Figure 10 shows the lidar return signals for two buoys, which clearly show a good signal-to-noise ratio.

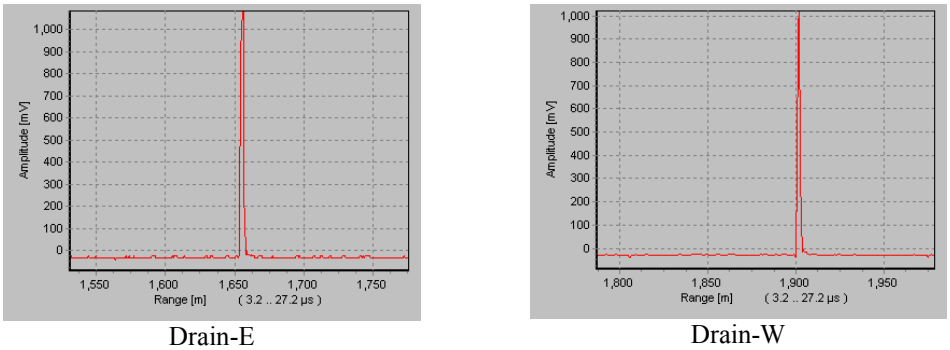

Drain-E Drain-W

Figure 10 Laser return signals of two buoys measured with the 1.5 µm lidar.

Since the lidar is eye-safe, we can also aim the system at manned platforms without risk of eye damage. Figure 11 shows that is it feasible to detect a small sailing boat at 3.4 km. Given the good signal-to-noise ratio, much larger ranges are possible. Ranges up to 10 km were achieved with this lidar at a NATO trial in Norway in the summer of 2007.[12]

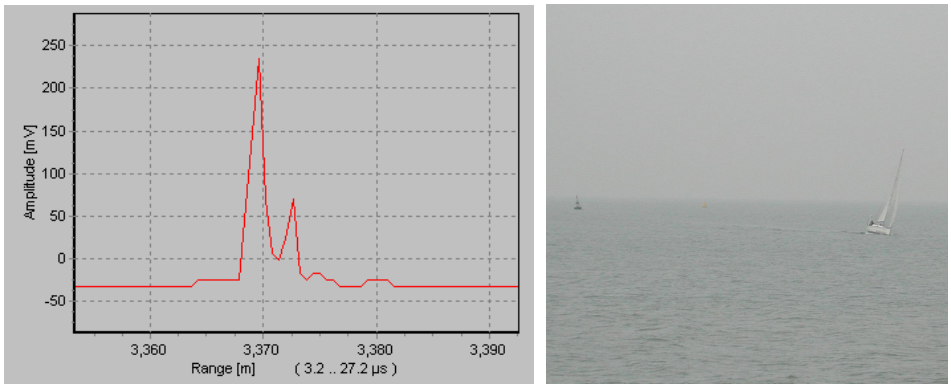

Figure 11 Laser range profile of a small sailing boat at 3.4 km. The photograph was taken at short range.

These encouraging results led to the development of a search-lidar demonstrator. Unfortunately, the high-power laser failed at the start of the system tests due to optical breakdown (system 3). Therefore, a much smaller laser with highly reduced power was used to test the system (system 4). A first test was at the laboratory in The Hague using two landmarks in the vicinity for testing the accuracy of the system. Figure 12 shows a photograph of these two landmarks (a radar sphere and a water tower) and the results from the search lidar. The detections of the lidar for the radar sphere clearly show the curved surface of the sphere. Since the beam is scanned in azimuth and elevation, the top part of the radar sphere is also plotted. It is clear that the range resolution is around 2 meter. This resolution is determined by the receiver and detection electronics. Results from the water tower show that a maximum range of 1500 meter has been achieved. However, there were some false alarms due to the low detection threshold.

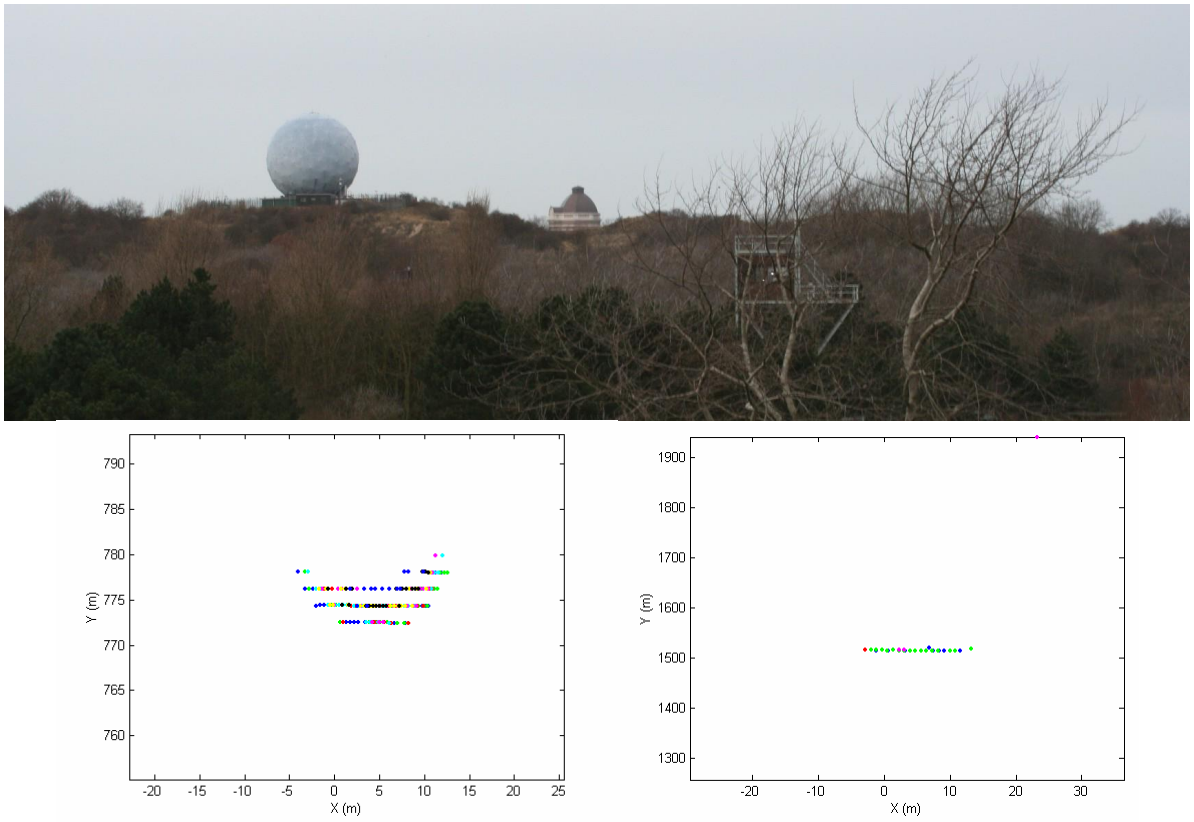

Figure 12: Photograph of a radar sphere and water tower (top). Search lidar detections are shown for the radar sphere (left) and for the water tower (right). Different colors indicate different elevation scans (however a single color represents more than one elevation).

Based on these successful results, the search-lidar demonstrator was stationed in the harbour of Scheveningen (near The Hague). Figure 13 shows a photograph of the harbour viewing the same part as the search lidar. The detections of the search lidar show the harbor wall and a passing ship (not in the photograph). The false alarms were negligible. The wind speed was about 6 Beaufort.

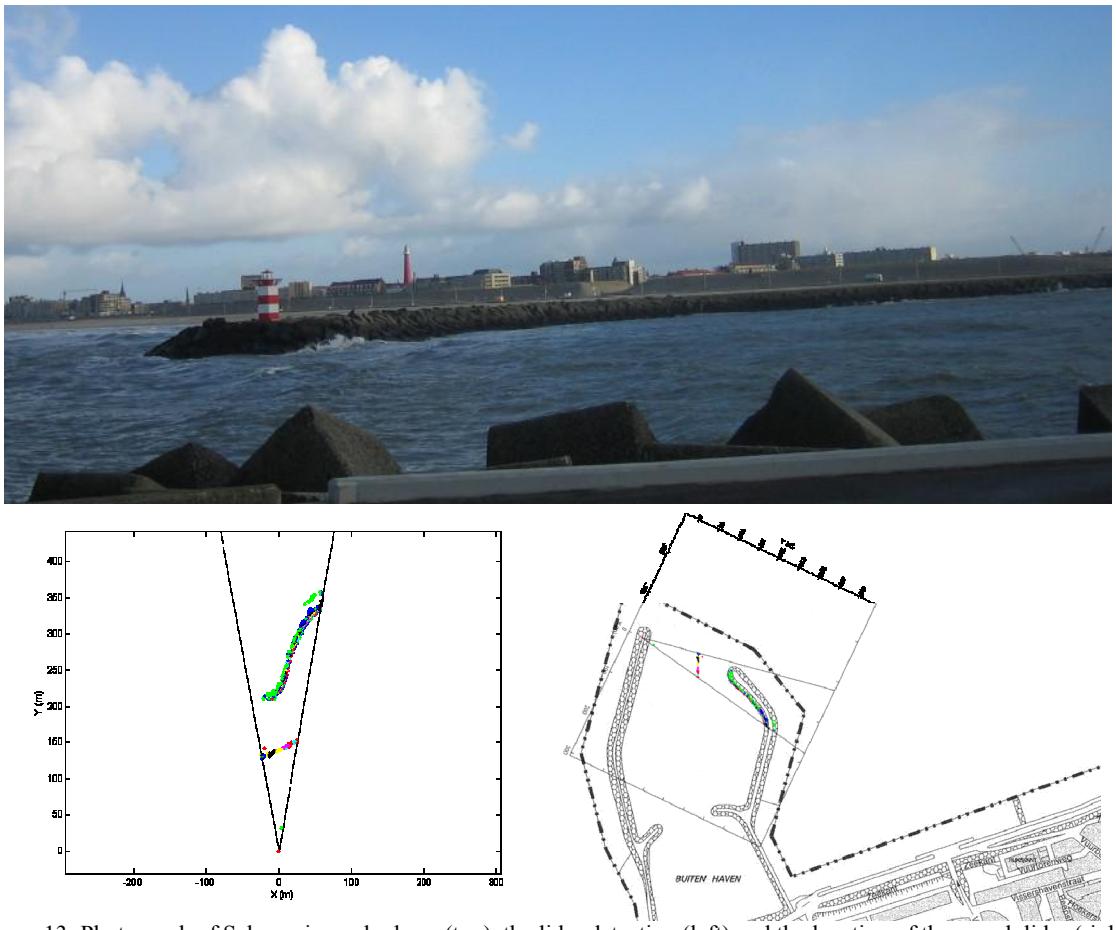

Figure 13: Photograph of Scheveningen harbour (top), the lidar detection (left) and the location of the search lidar (right).

The longest range that was tried was to a buoy at a range of 450 meter. Figure 14 shows photograph of the buoy from the position of the search-lidar demonstrator (top) and the detection of the search lidar. There were no false alarms and no detections were missed for the several scans that were performed.

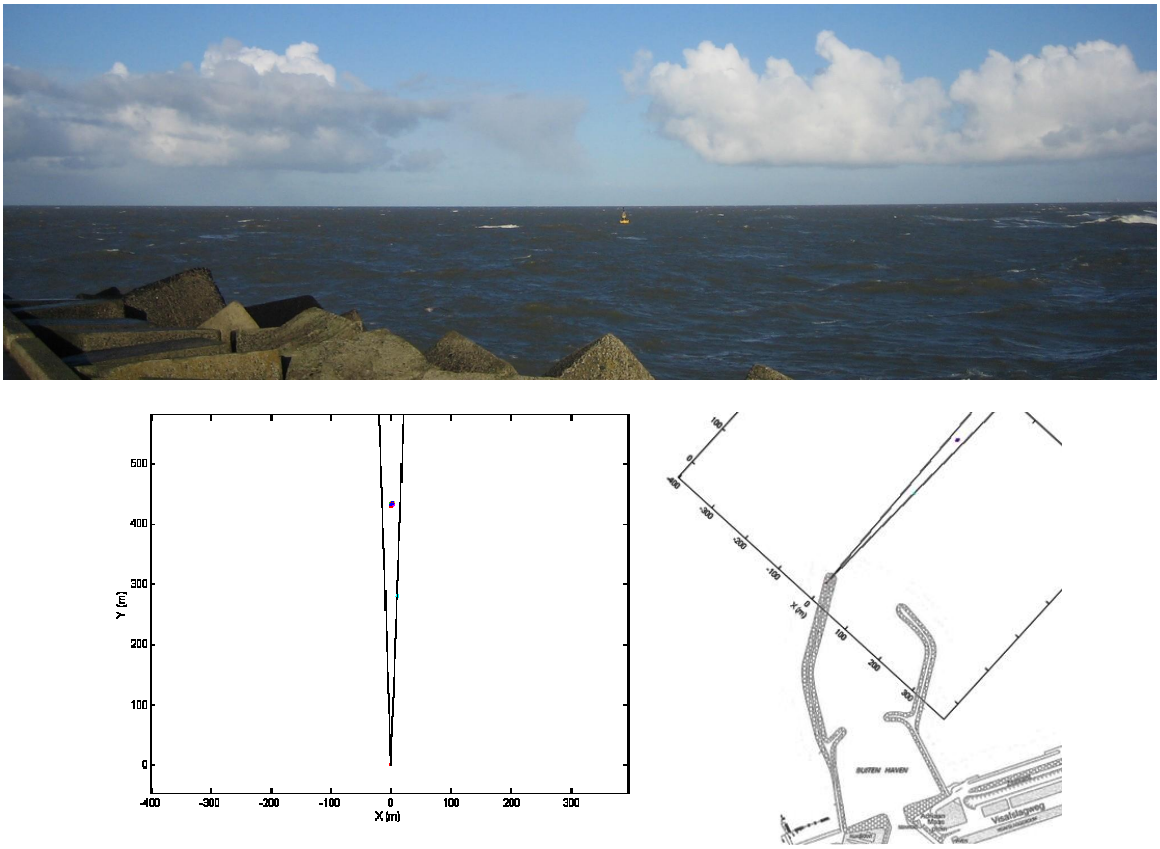

Figure 14: Photograph of the buoy (top), the lidar detection (left) and the pointing direction of the search lidar (right).

SEARCH TIME CALCULATION

We have developed a search-lidar demonstrator that has a high rep-rate with low pulse energy in order to demonstrate the feasibility of the concept. A crucial requirement is that the search time is short enough to detect sea-surface targets in time. Since the search space is limited (namely at small elevation angles below the horizon) and surface targets move relatively slow, this required search time is long enough for a search lidar to be feasible. Note that the search lidar is meant for slow moving surface targets that are difficult to detect for radar.

The search time is proportional to the number of laser pulses required for monitoring the sea surface around the search lidar position. For a horizontal scan (or azimuth scan) over angle θ, the number of pulses is

$$N_A = \frac{\theta}{\psi}, \tag{1}$$

where ψ is the laser beam divergence (and identical to the instantaneous field-of-view). For a full azimuth scan of 2π radians and a beam divergence of 1 mrad, we find that at least 6300 laser pulses are required. If the search lidar is mounted at a height h, then the geometrical horizon is a function of the radius of the earth R_E:

$$R_{GH} = \sqrt{2R_E h}\ . \tag{2}$$

For our low power system, a maximum range of 2 km is feasible. The corresponding minimum mounting height is 0.31 meter using equation (2) and the R_E of 6400 km. For a search lidar with a maximum range of around 10 km, the minimum mounting height for full range is 10 m. The elevation scan from minimum range R_{min} to the horizon needs the following number of laser pulses:

$$N_E = \frac{h}{R_{\min}\psi}\ . \tag{3}$$

A minimum range of 150 m means a depression angle of 2 mrad leading to two scans in the elevation direction based on the mounting height of 0.3 meter. Multiplying the number of horizontal and the vertical scans, we find a total number of 12.600 laser pulses.

The search time based on 12.600 laser pulses is around six seconds for our current low power 2 kHz laser. If we take into account that coastal surveillance will require a semi-circle scan, a search time of three seconds is obtained. This search time is sufficiently low to be applicable in coastal surveillance. Currently, the data acquisition of our search-lidar demonstrator is not fast enough to keep up with the 2 kHz laser. We hope to improve this in the near future.

SUMMARY AND CONCLUSIONS

We have presented a search-lidar demonstrator for detection of small sea-surface targets. Lidar experiments at the coast have shown very low (or no) reflections from the sea surface whereas strong reflections of small targets were measured up to ten kilometers. A combination of these two phenomena have led to the conclusion that it is possible to detect small targets on the sea surface, like buoys, periscopes, jet skies, swimmers and speed boats.

The results of a search-lidar demonstrator have been presented. The laser system that detects small targets at the sea surface at a range up to 2 km at good visibility is feasible with current laser technology. Such a system will have a search time of a few seconds. Longer ranges are also possible for instance up to 10 km. For these ranges, a higher power laser is required which is currently commercially available.

ACKNOWLEDGEMENTS

We thank Leo Böhmer of HITT Traffic for discussions on the application of coastal surveillance. We further thank Wim Pelt and Lt Menno Smeelen of the Netherlands Ministry of Defence for supporting this work in program V404.

REFERENCES

1. Kunz, G.J., Leeuw, G. de, Becker, E., and O'Dowd, C.D., "Lidar observations of atmospheric boundary layer structure and sea spray aerosol plumes generation and transport at Mace Head, Ireland (PARFORCE experiment)," Journal of Geophysical Research 107(D19), 11.1-11.14 (2002).
2. Kunz, G.J., et al., "Detection of small targets in a marine environment using laser radar", Proc. SPIE 5885, (2005).
3. Suits, G.H., "Natural sources", Chapter 3 in W.L.Wolfe and G.J. Zissis, Eds., *The infrared handbook* (1978).
4. Lillesand, T.M., and Kiefer, R.P., [Remote sensing and image interpretation], New York: John Wiley & Sons, (1973).
5. Rowan, L.C., Goetz, A.F.H., and Ashley, R.P., "Discrimination of hydro thermally altered and unaltered rocks in visible and near infrared multispectral images," Geophysics 42(3), 522-535, 1977.
6. Kahle, A.B., [Measuring spectra of arid lands, in Deserts and arid lands], El-Baz. F, Eds., pp. 195-217, Martinus Nijhoff Publishers, The Hague, The Netherlands, (1984).
7. Burnham, R.L., Kasinski, J.L., Marshall, L.R., "Eye-safe laser systems", US Patent No. 5181211, (1993).
8. G.A. Rines, D.G. Rines, P.F. Moulton, "Efficient, High-Energy, KTP Optical Parametric Oscillators Pumped with 1 μm Nd-Lasers", OSA Proceedings on Advanced Solid State Lasers, Washington DC, Vol. 20, pp. 461-463, (1994).
9. B. Boulanger, M.M. Fejer, "Study of gray-tracking at 1064, 532, and 355 nm", Applied Physics Letters 65 (19) (1994).
10. Heuvel, J.C. van den, et al., "Identification of Littoral Targets with a Laser Range Profiler". Proc. SPIE Vol. 6550 (2007).
11. Broek, A.C. van den, et al., "A multi-sensor scenario for coastal surveillance". Proc. SPIE Europe Remote Sensing, 17-20 September 2007 in Florence, Italy (2007).
12. Heuvel, J.C. van den, et al. "Experimental Validation of Ship Identification with a Laser Range Profiler", Proc. NATO MSS, March 2008 in Orlando, Florida USA.